Molecular and Cellular Biochemistry **279:** 105–112, 2005.
DOI: 10.1007/s11010-005-8227-y

Inorganic arsenic compounds cause oxidative damage to DNA and protein by inducing ROS and RNS generation in human keratinocytes

Wei Ding, Laurie G. Hudson and Ke Jian Liu

Program of Toxicology, College of Pharmacy, University of New Mexico Health Science Center, Albuquerque, NM, 87131, USA

Abstract

Arsenic is a naturally occurring element that is present in food, soil, and water. Inorganic arsenic can accumulate in human skin and is associated with increased risk of skin cancer. Oxidative stress due to arsenic exposure is proposed as one potential mode of carcinogenic action. The purpose of this study is to investigate the specific reactive oxygen and nitrogen species that are responsible for the arsenic-induced oxidative damage to DNA and protein. Our results demonstrated that exposure of human keratinocytes to trivalent arsenite caused the generation of 8-hydroxyl-2′-deoxyguanine (8-OHdG) and 3-nitrotyrosine (3-NT) in a concentration- and time-dependent manner. Pentavalent arsenate had similar effects, but to a significantly less extent. The observed oxidative damage can be suppressed by pre-treating cells with specific antioxidants. Furthermore, we found that pre-treating cells with *N*ω-nitro-L-arginine methyl ester (L-NAME), an inhibitor of nitric oxide synthase (NOS), or with 5,10,15,20-tetrakis (*N*-methyl-4′-pyridyl) porphinato iron (III) chloride (FeTMPyP), a decomposition catalyst of peroxynitrite, suppressed the generation of both 8-OHdG and 3-NT, which indicated that peroxynitrite, a product of the reaction of nitric oxide and superoxide, played an important role in arsenic-induced oxidative damage to both DNA and protein. These findings highlight the involvement of peroxynitrite in the molecular mechanism underlying arsenic-induced human skin carcinogenesis. (Mol Cell Biochem **279:** 105–112, 2005)

Key words: arsenic, DNA damage, keratinocytes, oxidative stress

Introduction

Arsenic is widely distributed in the environment and normally exists in two oxidative states: trivalent arsenite (As(III)) and pentavalent arsenate (As(V)). Environmental or occupational exposures to arsenic may result in both acute and chronic toxic effects in humans [1]. Dermatologic toxicities due to arsenic exposure are well documented. Arsenic accumulates in the skin and is associated with hyperkeratosis and acanthosis, pigmentation disorders, and skin cancers including basal cell carcinoma (BCC) and squamous cell carcinoma (SCC) [2–5]. Partly due to the lack of valid and reproducible animal models, the molecular mechanism(s) underlying arsenic-induced skin carcinogenesis remain unclear.

Reactive oxygen species (ROS) refers to a diverse group of reactive, short-lived, oxygen containing species, such as superoxide anion ($O_2^{\bullet -}$), hydrogen peroxide (H_2O_2), hydroxyl radical ($^{\bullet}OH$), singlet oxygen ($^1O_2$), and peroxyl radical ($LOO^{\bullet}$). Nitric oxide ($NO^{\bullet}$) and peroxynitrite ($ONOO^-$) are referred to as reactive nitrogen species (RNS). Our recent study has shown that exposure of human keratinocytes to arsenic leads to the formation of $O_2^{\bullet -}$ and H_2O_2 [6].

Generation of ROS is associated with a wide range of DNA damage including modification of bases and DNA

Address for offprints: K.J. Liu, College of Pharmacy, MSC09 5360, University of New Mexico, Albuquerque, NM 87131, USA (E-mail: jliu@unm.edu)

strand breaks. Alternatively, ROS can oxidize lipid or protein molecules to generate intermediates that react with DNA to form adducts. The DNA damage can lead to cell apoptosis or DNA mutations [7]; therefore, analysis of oxidative DNA damage in cells exposed to arsenic is necessary in order to better understand mechanisms contributing to arsenic-induced carcinogenesis. One of the major pathways of ROS-induced DNA damage involves attack at the C-8 position of 2′-deoxyguanine to form the 8-hydroxyl-2′-deoxyguanine (8-OHdG). The 8-OHdG has been shown to cause mis-pairing during DNA replication, giving rise to G to T conversion, and consequently the G:C → T:A mutation occurs. This is one of the most common mutations observed in selected codons in the H-*ras* proto-oncogene and the *p*53 tumor suppressor gene that are frequently mutated in human tumors [8, 9]. The formation of 8-OHdG is considered as an important biomarker of oxidative DNA damage [10].

When both $O_2^{\bullet -}$ and $NO^{\bullet}$ are generated in the cell, these two reactive species can react rapidly to form $ONOO^-$. Nitration on the 3-position of tyrosine is a major product of $ONOO^-$ attack on proteins. There is mounting evidence that nitration of tyrosine residues in proteins can profoundly alter protein function [11–14], suggesting that protein nitration may be fundamentally related to, and predictive of, oxidative cell injury. Furthermore, this nitrated residue can also be used as a diagnostic marker for the formation of $ONOO^-$ and indirectly, $O_2^{\bullet -}$ and $NO^{\bullet}$.

The purposes of this study are to investigate the oxidative damage to DNA and protein, using 8-OHdG and 3-NT as biomarkers, and to determine the specific reactive species that are responsible for these damages, after the exposure of the human keratinocytes to inorganic arsenic, both As(III) and As(V). The formation of 8-OHdG and 3-NT was sensitively and quantatively measured by the high performance liquid chromatography–electrochemical detection (HPLC–EC) assay.

Materials and methods

Materials

Sodium arsenite, sodium arsenate, deferoxamine mesylate salt, superoxide dismutase (SOD), catalase, *N*ω-nitro-L-arginine methyl ester (L-NAME), 3-nitrotyrosine (3-NT), 8-hydroxy-2′-deoxyguanine (8-OHdG), 2′-deoxyguanine (2′-dG), protease (XIV from *Streptomyces griseus*), potassium phosphate (monobasic), and sodium citrate were all obtained from Sigma (St. Louis, MO). 5,10,15,20-tetrakis (*N*-methyl-4′-pyridyl) porphinato iron(III) chloride (FeTMPyP) and Mn(III)tetrakis(1-methyl-4-pyridyl) porphyrin pentachloride (MnTMPyP) were purchased from Calbiochem (San Diego, CA). Nuclease P1 was obtained from US Biological (Swampscott, MA). The calf intestine alkaline phosphatase (CIAP) and CIAP buffer were obtained from Fermentas (Hanover, MD). RNase A was from Ambion (Austin, TX). The DNA extraction kit used was obtained from Wako Pure Chemical industry (Osaka, Japan). The 30000 Da and 3000 Da cutoff micro-filtration tubes were from Pall Life Science (East Hills, NY).

Cell culture and arsenic treatment

Human keratinocyte cell line (HaCaT) was generously provided by Dr Mitch Denning (Loyola University Medical Center, Maywood, IL). The HaCaT cells were maintained in Dulbecco's modified Eagle's medium F:12 HAM (DMEM F:12), supplemented with 10% newborn calf serum from Life Technologies/Gibco, four-fold concentration of MEM amino acids solution, 2 mM L-glutamine and antibiotics (penicillin, 100 U/ml and streptomycin, 50 μg/ml). The cells were cultured at 37 °C in 95% air/5% CO_2 humidified incubators.

Stock solutions of sodium arsenite and sodium arsenate at 10 mM were prepared in doubled-distilled water and sterilized by passing through a 0.22 μm syringe filter. The working concentration was prepared by diluting the stock with DME:F12 medium containing 0.1% bovine serum albumin (BSA). For all experiments involving incubation with arsenic, HaCaT cells were rinsed with phosphate-buffered saline (PBS) and placed into BSA medium containing different concentrations of arsenic indicated in the figures and figure legends.

Treatment of cells with antioxidants

Cells were treated with SOD and catalase according to Kessel *et al.* [15]. Briefly, stock copper/zinc SOD from bovine liver (Sigma, St. Louis, MO) was dissolved in double-distilled water, filtered through a 0.22 μm syringe filter and stored at −20 °C until use. A working solution of 400 U/ml was prepared fresh each time from stock solution by dilution in DME:F12 medium containing 0.1% BSA. Stock catalase solution was membrane filtered and diluted with medium to a final concentration of 5000 U/ml. The stock solutions of MnTMPyP and FeTMPyP were prepared in double-distilled water and filtered through a 0.22 μm syringe and diluted with medium to a working concentration of 5 μM. Stock solution of L-NAME was prepared in double distilled water after filtering through a 0.22 μm syringe and diluted to a working concentration of 1 mM. The final concentration of DMSO in the culture medium was 1% (v/v).

HPLC-EC detection of 8-OHdG

DNA extraction and hydrolysis procedures were performed according to the protocol by Helbock *et al.* [10] using the DNA extraction kit from Wako Pure Chemical industry (Osaka, Japan). Briefly, cell pellets were suspended in 1 ml of lysis buffer and then vortexed at moderate speeds for 30 s and then centrifuged for 20 s at 10,000 × *g* and 4 °C. The supernatant was discarded and replaced with 1 ml of fresh lysis buffer. The sample was vortexed and centrifuged again. The supernatant was discarded and 200 μl of enzyme solution was added, followed by 15 μl RNase A to a final concentration of 15 μg/ml. The sample was then incubated at 50 °C for 10 min. This first incubation was followed by the addition of 10 μl of proteinase solution to a final concentration of 0.75 mg/ml and further incubated at 50 °C for 50 min. During the second incubation, the samples were mixed by inversion every 10–15 min. The supernatant was then transferred to a fresh Eppendorf tube, 0.3 ml of NaI solution added and the sample mixed by repeated inversion. 2-Propanol (0.5 ml) was added and the sample mixed until 2–3 min after the first white DNA precipitate appeared. The sample was centrifuged at 10,000 × *g* for 5 min at ambient temperature, following which the supernatant was removed and the tube drained by inversion on absorbent paper. The pellet was washed with 1 ml of washing solution A. Following another centrifugation at 10,000 × *g* for 5 min at room temperature, the supernatant was aspirated and 1 ml of washing solution B added, the sample was centrifuged as before and the pellet immediately hydrolyzed as described below.

DNA hydrolysis

DNA samples were dissolved in 200 μl of 0.1 mM Desferal/20 mM sodium acetate, pH 4.8. This was accomplished by using a micropipette to dislodge and disperse the pellet, followed by addition of 4 μl 3.3 mg/ml nuclease P1, and hand agitation for 10 min. The samples were then incubated for 15 min at 70 °C. After the incubation was complete, 20 μl CIAP buffer was added to the sample mixture and mixed by inversion. Four micro liters of 1 U/μl of CIAP was then added. Samples were mixed well by slow inversion and then incubated for 1 h at 37 °C. Following incubation, pH of the hydrolyzed DNA was adjusted by adding 20 μl of 3 M sodium acetate buffer, pH 5.1. The samples were transferred to a 30,000-Da micro-filtration tube, and centrifuged for 30 min at 10,000 × *g* and 4 °C. The samples were then placed in auto-injector vials with low-volume inserts for HPLC-EC analysis.

HPLC-EC analysis of hydrolyzed DNA

The mobile phase consisted of methanol/50 mM KH_2PO_4 (5:95), and was filtered through 0.22 μM membrane filter.

HPLC was performed with a 15 cm × 4.6 mm, 3 μm LC-18-DB column (Supelco, Bellefonte, PA) using isocratic elution at a flow rate of 1.0 ml/min. The samples were analyzed by a separate UV model 520 from ESA (Chelmsford, MA) at 260 nm for dG and an electrochemical detection system linked in series for 8-OHdG. The electrochemical detector was an ESA (Chelmsford, MA) Model 5600 CoulArray. The oxidation potentials used to detect 8-OHdG were set at 0.1 and 0.4 V, respectively.

The amount of 8-OHdG in the injected sample was measured by EC detection and the amount of dG was measured by UV absorbance. The amount of 8-OHdG and dG in the sample was calibrated with respective standards, i.e., using authentic 8-OHdG and dG. The level of 8-OHdG in sample DNA was expressed as the number of 8-OHdG per 10^6 dG.

HPLC-EC detection of 3-NT

Protein extraction and hydrolysis

Protein extraction and hydrolysis procedures were performed according to the protocol by Crow *et al.* [16]. Briefly, 1 ml of 0.1 M NaOAc, pH 7.2 was added to the collected cell pellet. The samples were vortexed and sonicated (Branson Sonifier, Branson Corp., Danbury, CT) to disrupt the cells. The concentration of proteins in the samples was measurement by Bradford Assay (Biorad Laboratories, Richmond, CA). After cells were lysed, samples were centrifuged at 14,000 × *g* for 10 min at 4 °C. One milliliter acetonitrile was added to the supernatant, solutions were placed at 4 °C for 10 min and precipitates were gently pelleted by centrifugation at 3800 × *g* for 5 min. Supernatants were decanted and the pellets dissolved again in 0.1 M NaOAc, pH 7.2 at a final concentration of protein at 4 mg/ml. Twenty milligram per milliliter protease (XIV from *Streptomyces griseus*) dissolved in 0.1 M NaOAc, pH 7.2 were added to samples at a final ratio of 1:5 (w/w). The protease was prepared by dialysis in 1:500 0.1 M NaOAc, pH 7.2 for 3 days with daily buffer change. The samples were placed in 50 °C water bath for 18 h. All hydrolyzed mixtures were then transferred to a 3000 Da micro-filtration tube to prevent intact protease or undigested protein from being injected into the HPLC.

HPLC-EC analysis and calculation

All samples were analyzed on an ESA (Chelmsford, MA) CoulArray HPLC instrument equipped with 12 electrochemical cells (channels) utilizing platinum electrodes arranged in line and set to increase specified potentials between 100 and 870 mV [channel(potential): 1(100 mV); 2(170 mV); 3(240 mV); 4(310 mV); 5(380 mV); 6(450 mV); 7(520 mV); 8(590 mV); 9(660 mV); 10(730 mV); 11(800 mV); 12(870 mV)]. The analytical column was a TOSOHAAS (Mongtomeryville, PA) ODS 80-TM C-18 reverse phase

column and the mobile phase was 50 mM sodium citrate/5% methanol (v/v), pH 4.7. HPLC analysis was performed under isocratic conditions at a flow rate of 1.0 ml/min. 3-NT was analyzed by direct injection; tyrosine was analyzed after samples were diluted 1000-fold by mobile phase. Both 3-NT and TYR were detected by the EC detector and the level of 3-NT was expressed as the number of 3-NT per 100 tyrosine (TYR).

Statistics

Statistical analysis of data was carried out using Student's *t*-test. Differences between means were regarded as significant if $p < 0.05$ and significant differences were labeled by an asterisk (*).

Results

Generation of 8-OHdG by arsenic in human keratinocyte

Oxidative damage to DNA is postulated to be an important contributor to degenerative diseases including aging and cancer [17]. 8-OHdG is a particularly useful biomarker of oxidative DNA damage because it represents approximately 5% of the total oxidized bases that are known to occur in DNA [18], and also because it can be measured with excellent sensitivity using electrochemical detection [10]. In the present study, an HPLC-EC assay was used to detect the formation of oxidative DNA lesions in HaCaT cells treated with arsenic. Treatment of cells with different concentrations of As(III) for 24 h in BSA medium resulted in a concentration-dependent increase in 8-OHdG levels with a significant increase ($p < 0.05$) observed at 10 μM of As(III) (Fig. 1(A)). Treatment of cells with 20 μM As(III) for increasing periods of time resulted in a time-dependent increase in 8-OHdG level with a significant increase ($p < 0.05$) observed after 16 h incubation (Fig. 1B).

In order to determine the specific reactive species that are responsible for the formation of 8-OHdG, we have investigated the effects of various antioxidants and scavengers on the level of 8-OHdG. HaCaT cells were pre-incubated with 400 U/ml SOD (an antioxidant to $O_2^{\bullet -}$), 5000 U/ml catalase (decomposes H_2O_2), 5 μM MnTMPyP (a cell permeable SOD mimic), 1% DMSO (a scavenger of $^{\bullet}OH$), 1 mM L-NAME (an inhibitor of $NO^{\bullet}$ synthase (NOS)), or 5 μM FeTMPyP ($ONOO^-$ decomposition catalyst) for 30 min in BSA medium. Then As(III) was added to the medium to a final concentration of 20 μM and incubated at 37 °C for 24 h. Compared with cells treated with As(III) alone, preincubation of cells with SOD, MnTMPyP, catalase, and DMSO almost completely inhibited 8-OHdG formation induced by the As(III) treatment. Interestingly, L-NAME and FeTMPyP also partially decreased 8-OHdG level (Fig. 2). These results suggested that both $O_2^{\bullet -}$ and $NO^{\bullet}$ were involved in oxidative DNA damage and the formation of 8-OHdG.

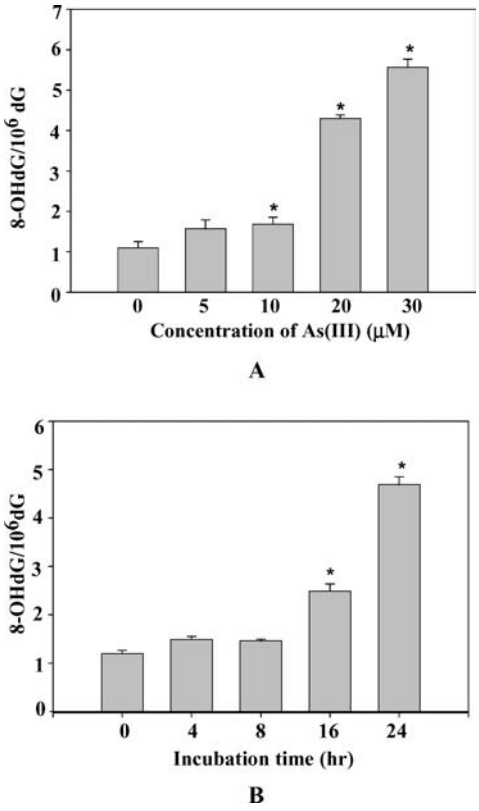

Fig. 1. As(III) induced 8-OHdG generation in a concentration- and time-dependent manner. (A) HaCaT cells were incubated with the indicated concentrations of As(III) in serum-free medium for 24 h. (B) HaCaT cells were incubated with 20 μM As(III) for the indicated times in BSA medium. Each experiment was repeated 3–5 times. Bars represent ±S.D., asterisk (*) represents $p < 0.05$.

In the present study, we compared the ability of As(V) to induce 8-OHdG generation in HaCaT cells. It is often stated that As(V) is less toxic than trivalent As(III). However, our results showed that treatment of cells with different concentrations of As(V) in BSA medium for 24 h could also induce 8-OHdG generation, with a significant increase evident at 20 μM As(V) exposure (Fig. 3). This concentration is greater than that of As(III) required to generate an equivalent response.

Generation of 3-NT by arsenic in human keratinocytes

When both $NO^{\bullet}$ and $O_2^{\bullet -}$ are generated, they can react rapidly to form $ONOO^-$. The resulting peroxynitrite can then react with L-tyrosine to form the chemically stable end product 3-NT. This nitrated residue has been used as a diagnostic

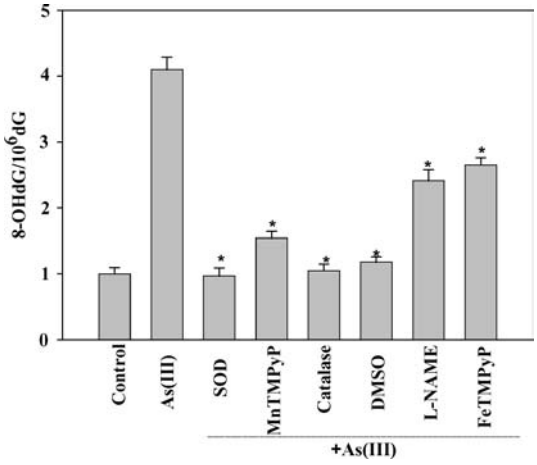

Fig. 2. Effects of antioxidants and scavengers on As(III)-induced 8-OHdG generation in HaCaT cells. HaCaT cells were pre-incubated with 400 U/ml SOD (an antioxidant to $O_2^{\bullet -}$), 5000 U/ml catalase (an antioxidant to H_2O_2), 5 μM MnTMPyP (a cell permeable SOD mimic), 1% DMSO (a scavenger of $^{\bullet}OH$), 1 mM L-NAME (an inhibitor of NOS), and 5 μM FeTMPyP (an $ONOO^-$ decomposition catalyst) for 30 min in BSA medium, then As(III) was added to the medium to a final concentration of 20 μM and incubated at 37 °C for 24 h. The experiment was repeated for 3–5 times, and bars represent ± S.D., asterisk (*) represents $p < 0.05$.

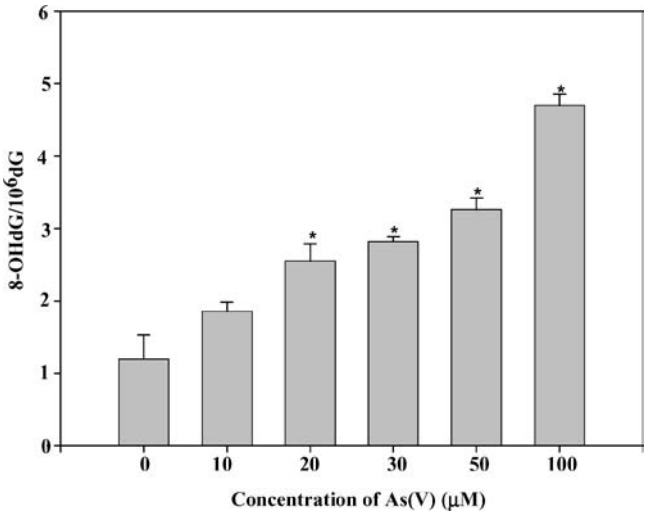

Fig. 3. As(V) induced generation of 8-OHdG. HaCaT cells were treated with 0, 10, 20, 30, 50 and 100 μM of As(V) at 37 °C for 24 h in BSA medium. The experiment was repeated three times, bars represent ±S.D., asterisk (*) represents $p < 0.05$.

marker for the formation of RNS *in vivo* and may compromise cellular functions by affecting enzymatic activities and components of the signal transduction cascades [19, 20]. Cells were treated using exactly the same experimental conditions as described in previous experiments. We observed that As(III) exposure in HaCaT cells resulted in a concentration-dependent 3-NT generation with a significant

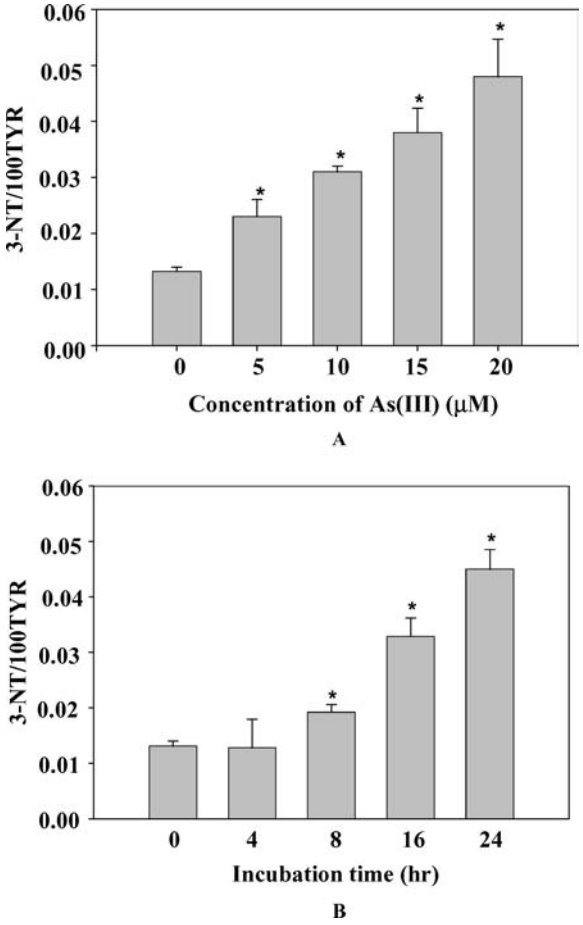

Fig. 4. As(III) induced generation of 3-NT in HaCaT cells. (A) Cells were incubated with 0, 5, 10, 15, and 20 μM of As(III) in BSA medium at 37 °C for 24 h. (B) Cells were incubated with 20 μM As(III) at 37 °C for 0, 4, 8, 16, and 24 h in BSA medium. Each experiment was repeated three times, bars represent ±S.D., asterisk (*) represents $p < 0.05$.

increase at 5 μM As(III) in 24 h (Fig. 4A). The generation of 3-NT was also time-dependent with a significant increase observed after cells were incubated with 20 μM As(III) for 8 h (Fig. 4B).

The effect of different ROS/RNS antioxidants and scavengers on the generation of 3-NT was also examined. Data in Fig. 5 shows the inhibitory effect of SOD (400 U/ml), MnTMPyP (5 μM), FeTMPyP (5 μM), and L-NAME (1 mM) on the generation of 3-NT induced by incubating HaCaT cells with 20 μM As(III) for 24 h. Suppression of 3-NT by the NOS inhibitor L-NAME suggested that $NO^{\bullet}$ was induced by As(III) through the action of NOS. Similarly, suppression of 3-NT by SOD and MnTMPyP suggested that $O_2^{\bullet -}$ was also involved in the protein damage. On the other hand, DMSO (1%), and catalase (5000 U/ml), the specific scavengers of $^{\bullet}OH$ and H_2O_2, had no suppressive effect on the formation of 3-NT, which indicate that $^{\bullet}OH$ and H_2O_2 were not involved

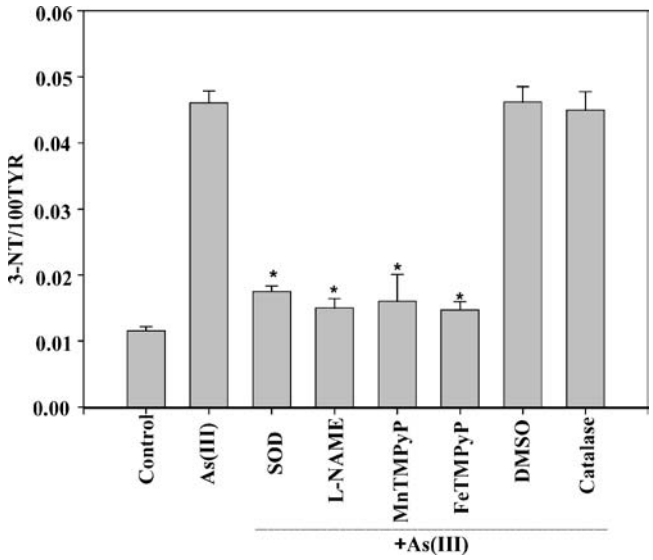

Fig. 5. Effects of antioxidants and scavengers on As(III)-induced 3-NT generation in HaCaT cells. HaCaT cells were pre-incubated with 400 U/ml SOD, 5000 U/ml catalase, 5 μM MnTMPyP, 5 μM FeTMPyP, 1% DMSO, or 1 mM L-NAME in BSA medium for 30 min at 37 °C, then As(III) was added to the medium to a final concentration of 20 μM and incubated at 37 °C for 24 h. The experiment was repeated 3–5 times, and bars represent ±S.D., asterisk (*) represents $p < 0.05$.

in the generation of 3-NT. The observed pattern of antioxidant inhibition suggests that generation of 3-NT is through the action of $ONOO^-$, and that $ONOO^-$ is formed through the reaction of $O_2^{\bullet-}$ and $NO^{\bullet}$.

The ability of As(V) to induce 3-NT in HaCaT cells was also examined. As(V) induced 3-NT generation in a concentration-dependent manner with a significant increase

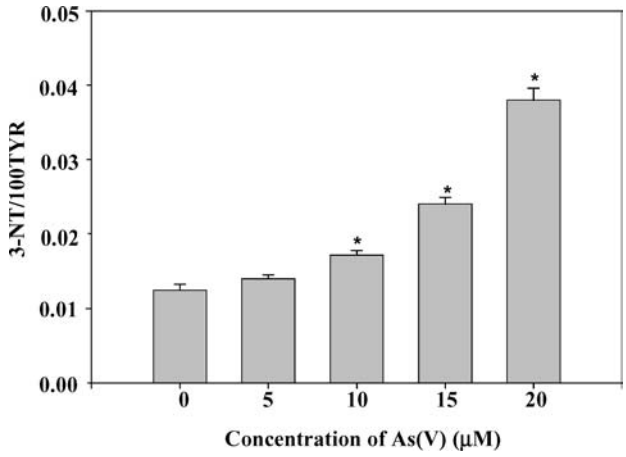

Fig. 6. As(V) induced 3-NT generation in HaCaT cells. HaCaT cells were incubated with 0, 5, 10, 15, and 20 μM of As(V) in BSA medium at 37 °C for 24 h. The experiment was repeated three times. Bars represent ±S.D., asterisk (*) represents $p < 0.05$.

observed after cells were incubated with 20 μM As(V) for 24 h (Fig. 6). As was observed with the generation of 8-OHdG, the concentration of As(V) required to generate an equivalent response was greater than that required for As(III).

Discussion

Although arsenic compounds are occasionally used as a medicine to treat acute promyelocytic leukemia (APL) [21], they are also known as human carcinogen [22]. The lack of suitable animal models hampers accurate risk assessment of the health effects of arsenic to humans. In the absence of an acceptable animal model, human keratinocytes, which represent a primary *in vivo* target of arsenic, provides a relevant and reasonable *in vitro* model to study the molecular mechanisms of arsenic carcinogenicity. In the present study, our data demonstrated that both ROS and RNS were generated after exposure of HaCaT cells to the inorganic arsenic compounds, both As(III) and As(V), based on the production of signature cellular damage. Furthermore, we found that $ONOO^-$, a powerful oxidant generated by the near diffusion-limited reaction of $NO^{\bullet}$ with $O_2^{\bullet-}$, played an important role in oxidative damage to both DNA and proteins. These results provide the direct evidence that $ONOO^-$ is the key species in arsenic-induced DNA and protein damage in the skin.

Recently oxidative stress is proposed as a possible mode of carcinogenic action of arsenic [23]. Mutagenesis and DNA damage caused by ROS contributes to the initiation of cancer. Among the ROS, neither $O_2^{\bullet-}$ nor H_2O_2 reacts with DNA bases, while $^{\bullet}OH$ generates a multiplicity of products from all four DNA bases and this pattern appears to be a diagnostic 'finger-print' of $^{\bullet}OH$ attack. The formation of 8-OHdG is often used as a biomarker to measure this attack [24]. When ROS cause damage to tumor suppressor genes or enhance the expression of proto-oncogenes, the cells may go on to become tumor cells [25]. Our results demonstrated that exposure of HaCaT cells to As(III) induced 8-OHdG generation in a concentration-dependent (Fig. 1A) and time-dependent (Fig. 1B) manner. In addition, we found that pre-treating cells with DMSO (a scavenger of $^{\bullet}OH$), SOD (an antioxidant to $O_2^{\bullet-}$), MnTMPyP (a cell permeable SOD mimic), catalase (an antioxidant to H_2O_2) suppressed the generation of 8-OHdG induced by As(III) (Fig. 2). These results further confirm the role of $^{\bullet}OH$ in the formation of 8-OHdG.

There is evidence demonstrating that 8-OHdG is generated following treatment of cells with $ONOO^-$ generators, which suggests that $ONOO^-$ derived from the reaction of $NO^{\bullet}$ and $O_2^{\bullet-}$ is involved in modifying the DNA bases [26, 27]. We found that pre-treating cells with L-NAME, an inhibitor of NOS, suppressed the generation of 8-OHdG, although not as much as DMSO, which implied that $NO^{\bullet}$ was partially involved in the DNA damage (Fig. 2). Pre-treating cells with

FeTMPyP, a recently developed $ONOO^-$ decomposition catalyst [28–30], also suppressed the 8-OHdG generation in a similar manner as L-NAME (Fig. 2). These results indicate that at least part of 8-OHdG formation was induced by the production of $ONOO^-$ inside the HaCaT cells. This finding is important since formation of 8-OHdG is usually associated with the generation of ROS, hence has often been used as a biomarker for ROS. Here we demonstrate that $ONOO^-$, derived from $NO^\bullet$ and $O_2^{\bullet-}$, contributes to the formation of 8-OHdG.

As(III) has been reported to increase $NO^\bullet$ production in human fetal brain [31] and in human umbilical vein endothelial cells, [32] and can also increase $NO^\bullet$ and $ONOO^-$ production in bovine aorta endothelial cells [24, 33]. As(V) has been reported to upregulate iNOS (inducible NO synthase) and to induce 3-NT generation in Swiss mice [34]. Souza *et al.* [35] also reported that after exposure of HaCaT cells to 200 μM As(III), the activation of eNOS (endothelial NO synthase) started 30 min after As(III) treatment and peaked at about 2 h. On the other hand, opposite effects of arsenic on $NO^\bullet$ production have been reported. For example, prolonged exposure to arsenic impaired production of endothelial $NO^\bullet$ in human blood [36]. As(III) also inhibited iNOS gene expression in rat pulmonary artery smooth muscle cells [37]. In vascular endothelial cells, no increased $NO^\bullet$ production was observed under environmental relevant exposure level of As(III) [38, 39]. In the present study, we demonstrated that As(III)-induced 3-NT generation in a time- and concentration-dependent manner (Fig. 4) with a significant increase observed after cells were incubated with as low as 5 μM As(III), a concentration that is generally considered nontoxic. Furthermore, pre-treating cells with SOD (an antioxidant to $O_2^{\bullet-}$), MnTMPyP (a cell-permeable SOD mimic), L-NAME (an inhibitor of NOS), FeTMPyP (a decomposition catalyst of $ONOO^-$), suppressed the generation of 3-NT after As(III) exposure. On the other hand, pre-treating cells with DMSO (a scavenger of $^\bullet OH$), and catalase (an antioxidant of H_2O_2), had no effect on 3-NT generation. Together, these results indicate that As(III) induced oxidative damage to protein is caused entirely by the production of $ONOO^-$ through the reaction of $NO^\bullet$ and $O_2^{\bullet-}$, and $^\bullet OH$ and H_2O_2 do not play a role in the observed protein damage.

As(V) is normally considered to be less toxic than As(III). In the present study, As(V) was found to be able to induce the generation of both 8-OHdG (Fig. 3) and 3-NT (Fig. 6) in a concentration-dependent manner, although at a significantly higher concentration than As(III) for the same effect. Since our earlier study has shown that As(V) did not produce a detectable increase of $O_2^{\bullet-}$ even at a concentration as high as 100 μM when HaCaT cells were exposed to As(V) for a short 20 min [6], we postulate that the observed DNA and protein damage by As(V) in this study is likely due to the fact that at an over-extended incubation time (such as 24 h), As(V) is slowly reduced to As(III) in a cellular environment. Therefore, the DNA and protein damage is most probably caused by the As(III) that was converted from As(V). Indeed, it has been reported that after human renal proximal tubule epithelial cells (HK-2) were incubated with As(V) for 24 h, more than half of As(V) was reduced to As(III) intracellularly [40], providing a strong support for our postulation.

In summary, using 8-OHdG and 3-NT as biomarkers, we find that inorganic arsenic, both As(III) and As(V), can induce oxidative damage to DNA and protein in human keratinocytes in a concentration- and time-dependent manner. These damages are caused by the arsenic-induced production of ROS and RNS, including $O_2^{\bullet-}$, H_2O_2, $^\bullet OH$, $NO^\bullet$, and $ONOO^-$. Our results also demonstrate that $ONOO^-$, a product of the reaction of $O_2^{\bullet-}$ and $NO^\bullet$, plays an important role in oxidative stress to both DNA and proteins. This implies that $ONOO^-$ production may be a crucial step in the mechanism of arsenic toxicity and carcinogenesis. These findings will contribute toward a better understanding of the molecular mechanism underlying arsenic-induced human skin carcinogenesis.

Acknowledgements

This research was supported in part by Grants from NIH (R01 ES012938, R01 AR42989, P20 RR15636, and P30 ES012022 Pilot Grant). Thanks to Ms Karen L. Cooper for her help in cell culture experiments. Mr Aaron Pritchard's assistance in preparing this manuscript was invaluable.

References

1. Edelman P: Environmental and workplace contamination in the semiconductor industry: Implications for future health of the workforce and community. Environ Health Perspect 86: 291–295, 1990
2. Shannon RL, Strayer DS: Arsenic-induced skin toxicity. Human Toxicol 8: 99–104, 1989
3. Norton W, Dunnette D: Health effects of environmental arsenic. Wiley and Sons, Inc., 1994
4. Schwartz RA: Premalignant keratinocytic neoplasms. J Am Ac Dermatol 35: 223–242, 1996
5. Schwartz RA: Arsenic and the skin. Int J Dermatol 36: 241–250, 1997
6. Shi H, Hudson LG, Ding W, Wang SW, Copper KL, Liu SM, Shi XL, Liu KJ: Arsenite causes DNA damage in keratinocytes via generation of hydroxyl radicals. Chem Res Toxicol 17: 871–878, 2004
7. Marnett LJ: Oxyradicals and DNA damage. Carcinogenesis 21: 361–370, 2000
8. Denissenko MF, Pao A, Tang M, Pfeifer G.P: Preferential formation of benzo[α]pyrene adducts at lung cancer mutational hotspots in p53. Science 274: 430–432, 1996
9. Colapietro AM, Goodell AL, Smart RC: Characterization of benzo-[α]pyrene-initiated mouse skin papillomas for Ha-ras mutations and protein kinase C levels. Carcinogenesis 14: 2289–2295, 1993

10. Helbock HJ, Beckman KB, Ames BN: 8-hydroxydeoxyguanosine and 8-hydroxyguanine as biomarkers of oxidative DNA damage. Meth Enzymol 300: 156–166, 1999
11. Haddad IY, Zhu S, Ischiropoulos H, Matalon S: Nitration of surfactant protein A results in decreased ability to aggregate lipids. Am J Physiol Lung Cell Mol Physiol 270: L281–L288, 1996
12. MacMillian-Crow LA, Crow JP, Kerby JD, Beckman JS, Thomson JA: Nitration and inactivation of manganese superoxide dismutase in chronic rejection of human renal allografts. Proc Natl Acad Sci USA 93: 11853–11858, 1996
13. Zhu S, Haddad IY, Matalon S: Nitration of surfactant protein A (SP-A) tyrosine residues results in decreased mannose binding ability. Arch Biochem Biophys 333: 282–290, 1996
14. Crow JP, Ye YZ, Strong M, Kirk M, Barnes S, Beckman JS: Superoxide dismutase catalyzes nitration of tyrosines by peroxynitrite in the rod and head domains of neurofilament-L. J Neurochem 69: 1945–1953, 1997
15. Kessel M, Liu SX, Xu A, Santella R, Hei TK: Arsenic induces oxidative DNA damage in mammalian cells. Mol Cell Biochem 234/235: 301–308, 2002
16. Crow JP: Measurement and significance of free and protein-bound 3-nitrotyrosine, 3-chlorotyrosine, and free 3-nitro-4-hydroxyphenylacetic acid in biologic samples: a high-performance liquid chromatography method method using electrochemical detection. Meth Enzymol 301: 151–160, 1999
17. Ames BN, Shigenaga MK, Hagen TM: Oxidants, antioxidants, and the degenerative diseases of aging. Proc Natl Acad Sci USA 90: 7915–7922, 1993
18. Dizdaroglu M: Oxidative damage to DNA in mammalian chromatin. Mutat Res 275: 331–342, 1992
19. Berlett BS, Friguet B, Yim MB, Chock PB, Stadman ER: Peroxynitrite-mediated nitration of tyrosine residues in *Escherichia coli* glutamine synthetase mimics adenylylation: relevance to signal transduction. Proc Natl Acad Sci USA 93: 1776–1780, 1996
20. Kong SK, Yim MB, Stadtman ER, Chock PB: Peroxynitrite disables the tyrosine phosphorylation regulatory mechanism: Lymphocyte-specific tyrosine kinase fails to phosphorylate nitrated cdc2(6–20)NH2 peptide. Proc Nal Acad Sci USA 93: 3377–3382, 1996
21. Zhang P: The use of arsenic trioxide (As_2O_3) in the treatment of acute promyelocytic leukemia. J Biol Regul Homeost Agents 13: 195–200, 1999
22. NRC: National Research Council Report: Arsenic in the drinking water, National Academy Press, Washington, DC, 2001, pp 6975–7066
23. Kitchin KT: Recent advances in arsenic carcinogenesis: modes of action, animal model system, and methylated arsenic metabolites. Toxicol Appl Pharmacol 172: 249–261, 2001
24. Wiseman H, Halliwell B: Damage to DNA by reactive oxygen and nitrogen species: Role in inflammatory disease and progression to cancer. Biochem J 313: 17–29, 1996
25. Liu F, Jan KY: DNA damage in arsenite- and cadmium-treated bovine aortic endothelial cells. Free Radic Biol Med 28: 55–63, 2000
26. Kim HW, Murakami A, Williams MV, Ohigashi H: Mutagenicity of reactive oxygen and nitrogen species as detected by co-culture of activated inflammatory leukocytes and AS52 cells. Carcinogenesis 24: 235–241, 2003
27. Hattori Y, Nishigori C, Tanaka T, Uchida K, Nikaido O, Osawa T, Hiai H, Iamnura S, Toyokuni S: 8-hydroxy-2′-deoxyguanosine is increased in epidermal cells of hairless mice after chronic ultraviolet B exposure. J Invest Dermatol 107: 733–737, 1997
28. Xie Z, Wei M, Morgan TE, Fabrizio P, Han Derick, Finch CE, Longo VD: Peroxynitrite mediates neurotoxicity of amyloid β-peptide$_{1-42}$ and lipopolysaccharide-activated microglia. J Neurosci 22: 3484–3492, 2002
29. Nagle MR, Cotter MA, Caneron NE: Effects of peroxynitrite decomposition catalyst, FeTMPyP, on function of corpus cavernosum from diabetic mice. Eur J Pharmacol 502: 143–148, 2004
30. Sharma SS, Munusamy S, Thiyagarajan M, Kaul CL: Neuroprotective effect of peroxynitrite decomposition catalyst and poly(adenosine diphosphate-ribose) polymerase inhibitor alone and in combination in rats with focal cerebral ischemia. J Neurosurg 101: 669–675, 2004
31. Chattophadhyay S, Bhaumik S, Chrudhury AN, DasGupta S: Arsenic induced changes in growth development and apoptosis in neonatal and adult brain cells in vivo and in tissue culture. Toxicol Lett 128: 73–84, 2002
32. Kao YH, Yu CL, Chang LW, Yu HS: Low concentrations of arsenic vascular endothelial growth factor and nitric oxide release and stimulate angiogenesis *in vitro*. Chem Res Toxicol 16: 460–468, 2003
33. Bunderson M, Coffin JD, Beall HD: Arsenic induces peroxynitrite generation and cyclooxygenase-2 protein expression in aortic endothelial cells: possible role in atherosclerosis. Toxicol Appl Pharmacol 184: 11–18, 2002
34. Waalkes MP, Keeper LK, Diwan BA: Induction of proliferative lesions of the uterus, testes, and liver in Swiss mice given repeated injections of sodium arsenate: Possible estrogenic mode of action. Toxicol Appl Pharmacol 166: 24–35, 2000
35. Souza K, Maddock, DA, Zhang Q, Chen J, Chiu C, Mehta S, Wan Y: Arsenite activation of P13/AKT cell survival pathway is mediated by p38 in culture human keratinocytes. Mol Med 7: 767–772, 2001
36. Pi J, Kumagai Y, Sun G, Uamauchi H, Yoshida T, Iso H, Endo A, Yu L, Yuki K, miyauchi T, Shimojo N: Decreased serum concentrations of nitric oxide metabolites among Chinese in an endemic area of chronic arsenic poisoning in inner Mongolia. Free Radic Biol Med 28: 1137–1142, 2000
37. Wong HR: Expression of iNOS in cultured rat pulmonary artery smooth muscle cells is inhibited by the heat shock response. Am J Physiol 269: L843–L848, 1995
38. Barchowsky A, Klei LR, Dudek EJ, Swartz HM, James PE: Stimulation of reaction oxygen, but not reactive nitrogen species, in vascular endothelial cells exposed to low levels of arsenite. Free Radic Biol Med 27: 1405–1412, 1999
39. Christodoulides N: Vascular smooth muscle cell heme oxygenases generate guanylyl cyclase-stinulatory carbon monoxide. Circulation 91: 2306–2309, 1995
40. Peraza MA, Carter DE, Gandolfi AJ: Toxicity and metabolism of subcytotoxicity inorganic arsenic in human renal proximal tubule epithelial cells (HK-2). Cell Biol Toxicol 19: 253–264, 2003